

Finite Element Computation of KPP Front Speeds in Cellular and Cat's Eye Flows

Lihua Shen · Jack Xin · Aihui Zhou

Received: 9 January 2012 / Revised: 23 July 2012 / Accepted: 28 August 2012 /
Published online: 12 September 2012
© Springer Science+Business Media, LLC 2012

Abstract We compute the front speeds of the Kolmogorov-Petrovsky-Piskunov (KPP) reactive fronts in two prototypes of periodic incompressible flows (the cellular flows and the cat's eye flows). The computation is based on adaptive streamline diffusion methods for the advection-diffusion type principal eigenvalue problem associated with the KPP front speeds. In the large amplitude regime, internal layers form in eigenfunctions. Besides recovering known speed growth law for the cellular flow, we found larger growth rates of front speeds in cat's eye flows due to the presence of open channels, and the front speed slowdown due to either zero Neumann boundary condition at domain boundaries or frequency increase of cat's eye flows.

Keywords KPP front speeds · Cellular and cat's eye flows · Eigenvalue problems · Adaptive streamline diffusion finite element method

1 Introduction

Front propagation in fluid flows is a ubiquitous nonlinear phenomenon that arises in pre-mixed turbulent combustion and reactive transport in porous media among other applications [8, 12, 13, 19, 24, 25, 29, 32, 33, 35]. A fundamental problem is to characterize, bound and compute large scale front speeds. Though the problem is challenging in general for complex

L. Shen (✉)
School of Mathematics, Capital Normal University, Beijing 100048, China
e-mail: shenlh@lsec.cc.ac.cn

J. Xin
Department of Mathematics, University of California at Irvine, Irvine, CA 92697, USA
e-mail: jxin@math.uci.edu

A. Zhou
LSEC, Institute of Computational Mathematics and Scientific/Engineering Computing, Academy of Mathematics and Systems Science, Chinese Academy of Sciences, Beijing 100190, China
e-mail: azhou@lsec.cc.ac.cn

flows, much progress has been made lately for the Kolmogorov-Petrovsky-Piskunov (KPP) reactive fronts in the large amplitude regime of steady periodic incompressible flows [1, 2, 23, 27, 36]. The prime example is the two dimensional cellular flows consisting of periodic array of vortices. The KPP equation is:

$$u_t = \kappa \Delta_z u + \mathbf{B}(z) \cdot \nabla_z u + \frac{1}{\tau_r} f(u), \quad z \in \mathbb{R}^n, \quad t > 0, \tag{1.1}$$

where κ and τ_r are two positive constants, \mathbf{B} is a given steady incompressible 2π -periodic velocity field; $f(u) = u(1 - u)$, the so called KPP nonlinearity.

In this paper, we shall carry out a numerical study of KPP front speeds of Eq. (1.1) in a two dimensional infinite strip $\mathbb{R}^1 \times [0, L]$; so $n = 2$, $z = (x, y)$, $x \in \mathbb{R}^1$, $y \in [0, L]$. The boundary condition at $y = 0, L$ is either zero Neumann or periodic. If the initial data for u is nonnegative and front-like (approaching zero and one rapidly enough as $x \rightarrow \pm\infty$), large time behavior of u is a propagating front along x . We will denote the KPP front speed as μ which admits a variational characterization in terms of principal eigenvalue of an associated linear operator [6, 33]. More precisely, let $\Omega = [0, 2\pi] \times [0, L]$, and for each fixed λ , we consider the classical principal eigenvalue problem of (H, ϕ) with either zero Neumann boundary condition at $y = 0, L$ or L -periodic in y :

$$\begin{cases} \kappa \Delta \phi + (2\kappa \lambda \mathbf{e} + \mathbf{B}(x, y)) \cdot \nabla \phi + [\kappa \lambda^2 + \lambda \mathbf{e} \cdot \mathbf{B}(x, y) + \tau^{-1} f'(0)] \phi = H(\lambda) \phi, \\ \phi|_{x=0} = \phi|_{x=2\pi}; \quad \frac{\partial \phi}{\partial \mathbf{n}}|_{y=0, L} = 0 \text{ or } \phi|_{y=0} = \phi|_{y=L}. \end{cases} \tag{1.2}$$

Here \mathbf{n} is the outer normal vector, $\mathbf{e} = (1, 0)$, and $\mathbf{B}(x, y)$ is either a 2-dimensional cellular flow

$$\mathbf{B}(x, y) = (-\sin x \cos y, \cos x \sin y) \tag{1.3}$$

or a periodic perturbation of the cellular flow ($\delta > 0$ is a constant)

$$\mathbf{B}(x, y) = (-\sin x \cos y, \cos x \sin y) + \delta(\cos x \sin y, -\sin x \cos y) \tag{1.4}$$

the so called cat’s eye flow. Both cellular flow and cat’s eye flows have been studied extensively for flow enhanced diffusion and dynamo problems [11, 16].

The KPP front speed is given by:

$$\mu = \inf_{\lambda > 0} \frac{H(\lambda)}{\lambda}, \tag{1.5}$$

where $H(\lambda)$ is the largest eigenvalue of (1.2). This variational formula makes possible accurate and efficient computation of KPP front speeds without direct simulation of the time-dependent reaction-diffusion-advection equation (1.1). Even for random flows, computation based on variants of (1.5) are performed in [22, 28]. In [28], the present authors initiated a numerical study for KPP front speeds in random shear flows using two-scale finite element methods. In this paper, we shall study KPP front speeds in periodic cellular flows and cat’s eye flows based on an adaptive streamline diffusion finite element method. If the flow field is scaled as $\mathbf{B}(x, y) \rightarrow A \cdot \mathbf{B}(x, y)$ for a positive constant A , we are interested in the dependence of front speed on A when A is large. For cellular flows and propagation in the entire plane, asymptotic result [2, 23] says that $\mu(A) = O(A^{1/4})$ as $A \gg 1$ independent of the direction of propagation (isotropic). For cat’s eye flows and propagation in the entire plane, front speeds are anisotropic [34]: $\mu(A) = O(1)$ along direction $(-1, 1)/\sqrt{2}$, $\mu(A) = O(A)$

along any other direction. At large A , the eigenfunction ϕ develops internal layers, for which an adaptive finite element method is appropriate. It is not known at what threshold value the asymptotic regime is entered. This is what we shall study numerically as well.

The rest of the paper is organized as follows. In Sect. 2, we give a brief overview of asymptotic theory of KPP front speeds in the large A limit. In Sect. 3, we present adaptive and streamline diffusion finite element methods for computation of eigenvalue problem (1.2). In Sect. 4, we present numerical results on KPP front speeds. We first recover the known growth law $A^{1/4}$ for cellular flows with our method at $A \sim 10^3$, then show findings of increased KPP front speeds in cat’s eye flows due to the presence of open channels. Though our numerical results are for front speeds in $(1, 0)$, a fast direction, the linear growth asymptotic regime of cat’s eye flow is not yet reached based on the A values up to 10^3 . Instead, we observed intermediate growth exponents in $(1/4, 1)$. The threshold value of A to enter the theoretical scaling regime of front speeds in cat’s eye flows appears to be much larger than that for cellular flows. We also compare front speeds under zero Neumann and periodic boundary conditions for cat’s eye flows. We found that zero Neumann boundary condition may slow down front speed at large A . In contrast, periodic boundary condition always enhances front speed so that the growth law observed is $O(A^p)$, $p \in (1/4, 1]$ due to the presence of channels from periodic perturbation ($\delta > 0$). We also found that increasing the oscillation frequency of cat’s eye flows in the domain slows down the front speed growth in A . In Sect. 5, we conclude with remarks on future work of computing KPP front speeds in three dimensional periodic steady flows in cylindrical domains. Acknowledgments are in Sect. 6.

2 Asymptotic Theory: An Overview

KPP front speed in two dimensional periodic steady flows in the entire plane has been actively studied in recent years in the regime of large flow amplitude or when the flow field B is scaled up by a large factor $A \gg 1$. The first type of result concerns μ in cellular flows at large A , $\mu(A) \sim O(A^{1/4})$, [2, 23]. The second type of result [34] is on anisotropic behavior of the front speeds in cat’s eye flows at large A : $\mu(A) = O(1)$ in the direction $(-1, 1)/\sqrt{2}$ and $O(A)$ in any other direction. For more general two dimensional periodic flows, explicit growth exponent is difficult to find, however $\mu(A)$ is related to the effective diffusivity in the same flow in case of (1.2) with periodic boundary condition in y . Consider the advection-diffusion equation:

$$p_t = \kappa \Delta p + A \mathbf{B}(z) \cdot \nabla_z p, \tag{2.1}$$

whose long-time behavior is governed by the effective diffusion equation:

$$\bar{p}_t = \sum_{i,j=1}^n \sigma_{ij}(A) \bar{p}_{z_i, z_j}. \tag{2.2}$$

The z -independent diffusivity matrix $\sigma(A)$ is given by the cell problem as follows. For $e \in \mathbb{R}^n$, let $\chi_e(\xi)$ be the periodic mean-zero solution of:

$$\kappa \Delta_\xi \chi_e + A \mathbf{B} \cdot \nabla_\xi \chi_e = A \mathbf{B} \cdot e, \tag{2.3}$$

on the n -dimensional unit torus \mathbb{T}^n . The matrix $\sigma(A)$ is:

$$e \cdot \sigma(A) e' = \int_{\mathbb{T}^n} (\nabla \chi_e + e) \cdot (\nabla \chi_{e'} + e') d\xi = e \cdot e' + \int_{\mathbb{T}^n} \nabla \chi_e \cdot \chi_{e'} d\xi, \tag{2.4}$$

for any $e, e' \in \mathbb{R}^n$. The effective diffusivity in the direction e is:

$$D_e(A) = e \cdot \sigma(A)e = 1 + \int_{\mathbb{T}^n} |\nabla \chi_e|^2 d\xi. \tag{2.5}$$

The front speed μ_e along direction e over the entire plane is bounded from above and below by constant times $\sqrt{D_e}$. It is proved in [27] that for some constant independent of (A, \bar{B}, f, e) :

$$\frac{\sqrt{f'(0)}}{C(1 + \sqrt{f'(0)})} \leq \frac{\mu_e(A)}{\sqrt{D_e(A)}} \leq C\sqrt{f'(0)}(1 + \sqrt{f'(0)}). \tag{2.6}$$

Hence information on $D_e(A)$ can be transferred to $\mu_e(A)$. For example, it is known [16] that cat’s eye flows contain channels of width $O(\delta)$ along direction $d = (1, 1)/\sqrt{2}$ where maximal diffusivity enhancement takes place, $D_d(A) = O(A^2)$ for any fixed δ . This implies that $\mu_d(A) = O(A)$. Along the orthogonal direction $d_\perp = (-1, 1)/\sqrt{2}$, closed streamlines in the eddies cause minimal diffusivity enhancement, $D_{d_\perp}(A) = O(1)$, so $\mu_{d_\perp}(A)$ is uniformly bounded in $A \gg 1$. Along any other direction, one has a mixture of fast and slow transport. It is only recently proved that the growth law away from the slow direction is $O(A)$ [34], or the fast transport eventually wins as $A \rightarrow +\infty$. We shall compute front speeds along a fast direction $(1, 0)$ under both zero Neumann and periodic boundary conditions in y . It is worth pointing out that the inequality (2.6) is false in three and higher dimensions [37]. In particular, it remains to discover the relationship between $\mu_e(A)$ and $D_e(A)$ in three space dimensions through numerical and analytical studies. We refer to [7, 36] for first integral type criteria, [34] for periodic orbits and invariant measure type criteria on linear or sublinear growth of front speeds in A .

3 Numerical Problem and Methods

For simplicity, let $L = 2\pi$ and consider the principal eigenvalue problem over domain $\Omega = [0, 2\pi] \times [0, 2\pi]$:

$$\begin{cases} \kappa \Delta \phi + (2\kappa \lambda \mathbf{e} + \mathbf{B}(x, y)) \cdot \nabla \phi + [\kappa \lambda^2 + \lambda \mathbf{e} \cdot \mathbf{B}(x, y) + \tau^{-1} f'(0)] \phi = H(\lambda) \phi, \\ \phi|_{x=0} = \phi|_{x=2\pi}; \quad \frac{\partial \phi}{\partial \mathbf{n}}|_{y=0, 2\pi} = 0, \text{ or } \phi|_{y=0} = \phi|_{y=2\pi}; \end{cases} \tag{3.1}$$

where $\kappa = 1.0$, $\tau = 2.0$. We shall apply and compare the standard finite element method, the streamline diffusion method, the upwind finite difference method, and an adaptive streamline diffusion method for computing (3.1).

The streamline diffusion method was originally proposed by Hughes and Brooks [17] for solving a boundary value problem. Starting with Nävert [21], it was then analyzed by Johnson and his co-workers (see, e.g., [18, 26] and references cited therein). The streamline diffusion method has been successfully applied to various problems, e.g., the model problems of many fluid flows including incompressible Navier-Stokes equations and diffusion-convection-reactive equations, the model problems in physics like semiconductor device [26], etc. However, to our best knowledge, there is no work applying the streamline diffusion method to solve an eigenvalue problem. We see also that adaptive finite element methods have been extensively studied since Babuška and Vogelius [4] gave an analysis of an adaptive finite element method for linear symmetric elliptic problems in one dimension. We refer to [15] for an adaptive streamline diffusion method for the stationary convection-diffusion (boundary value) problem and [14, 20, 30] and references cited therein for adaptive finite element method for linear eigenvalue problems.

Remark 3.1 It is open whether we are able to get the convergence properties for either the standard finite element method or a streamline diffusion method for eigenvalue problem reflecting the dependency of the parameter.

To simplify the presentation, we denote $\tilde{\mathbf{B}} = (\tilde{B}_x, \tilde{B}_y) = 2\kappa\lambda\mathbf{e} + \mathbf{A}\mathbf{B}(x, y)$, and $\tilde{C} = \kappa\lambda^2 + \lambda\mathbf{Ae} \cdot \mathbf{B}(x, y) + \tau^{-1}f'(0)$. The first equation of (3.1) has the form

$$\kappa \Delta \phi + \tilde{\mathbf{B}} \cdot \nabla \phi + \tilde{C} \phi = H(\lambda)\phi. \tag{3.2}$$

If the boundary condition is $\phi|_{x=0} = \phi|_{x=2\pi}, \frac{\partial \phi}{\partial \mathbf{n}}|_{y=0,2\pi} = 0$, we define

$$a(w, v) = -(\kappa \nabla w, \nabla v) + (\tilde{\mathbf{B}} \cdot \nabla w, v) + (\tilde{C} w, v) + \int_{x=0,2\pi} \kappa v \nabla w \cdot \mathbf{n} ds, \quad \forall w, v \in H^1(\Omega) \tag{3.3}$$

and

$$V = \{v \in H^1(\Omega) : v|_{x=0} = v|_{x=2\pi}\}$$

where (\cdot, \cdot) denotes the inner product in $L^2(\Omega)$. If the boundary condition is $\phi|_{x=0} = \phi|_{x=2\pi}, \phi|_{y=0} = \phi|_{y=2\pi}$, we define

$$a(w, v) = -(\kappa \nabla w, \nabla v) + (\tilde{\mathbf{B}} \cdot \nabla w, v) + (\tilde{C} w, v) + \int_{\partial \Omega} \kappa v \nabla w \cdot \mathbf{n} ds, \quad \forall w, v \in H^1(\Omega) \tag{3.4}$$

and

$$V = \{v \in H^1(\Omega) : v|_{x=0} = v|_{x=2\pi}, v|_{y=0} = v|_{y=2\pi}\}.$$

The variational form for Eq. (3.1) is as follows: Find $(H, \phi) \in \mathbb{R} \times V$ such that

$$a(\phi, v) = H(\phi, v), \quad \forall v \in V. \tag{3.5}$$

3.1 Standard Finite Element Method

Let T_h be a shape regular conforming triangular finite element mesh over Ω with size h . Denote the linear finite element space

$$S_h = \{p \in H^1(\Omega) : p|_{\tau} \text{ is piecewise linear, } \forall \tau \in T_h\}$$

and let

$$V_h = S^h \cap V.$$

The standard finite element discretization for (3.5) is: Find $(H_h, \phi_h) \in \mathbb{R} \times V_h$ such that

$$a(\phi_h, v) = H_h(\phi_h, v), \quad \forall v \in V_h. \tag{3.6}$$

The convergence and error estimates of approximations of (3.6) can be derived from [3] when the coefficients/parameters of (3.1) are of the same scale (see also [5]).

3.2 Upwind Finite Difference Method (Upwind FDM)

Assume that finite element mesh T_h is rectangular. Let $\{(x_i, y_j)\}$ ($i, j = 1, \dots, N$) be the grid points of the mesh. At the interior grid points (x_i, y_j) ,

$$\kappa(\Delta\phi)(x_i, y_j) + (\tilde{\mathbf{B}} \cdot \nabla\phi)(x_i, y_j) + (\tilde{C}\phi)(x_i, y_j) = H\phi(x_i, y_j). \tag{3.7}$$

Let $\phi(x_i, y_j)$ be approximated by ϕ_{ij} ($i, j = 1, 2, \dots, N$). On the left hand side of (3.7), we discretize the first term using center difference scheme as follows:

$$\Delta\phi(x_i, y_j) \approx \frac{\phi_{i-1,j} + \phi_{i+1,j} + \phi_{i,j-1} + \phi_{i,j+1} - 4\phi_{ij}}{h^2}. \tag{3.8}$$

The one order upwind scheme [9, 10] for the x direction of the second term is

$$\begin{cases} \frac{\partial\phi}{\partial x}(x_i, y_j) \approx \frac{\phi_{ij} - \phi_{i-1,j}}{h}, & \text{if } \tilde{B}_x > 0, \\ \frac{\partial\phi}{\partial x}(x_i, y_j) \approx \frac{\phi_{i+1,j} - \phi_{i,j}}{h}, & \text{if } \tilde{B}_x < 0. \end{cases} \tag{3.9}$$

Similarly, for the y direction,

$$\begin{cases} \frac{\partial\phi}{\partial y}(x_i, y_j) \approx \frac{\phi_{ij} - \phi_{i,j-1}}{h}, & \text{if } \tilde{B}_y > 0, \\ \frac{\partial\phi}{\partial y}(x_i, y_j) \approx \frac{\phi_{i,j+1} - \phi_{i,j}}{h}, & \text{if } \tilde{B}_y < 0. \end{cases} \tag{3.10}$$

The two order upwind schemes [9, 10] for the x and y directions of the second term are as follows:

$$\begin{cases} \frac{\partial\phi}{\partial x}(x_i, y_j) \approx \frac{1}{h}(\frac{3}{2}\phi_{ij} - 2\phi_{i-1,j} + \frac{1}{2}\phi_{i-2,j}), & \text{if } \tilde{B}_x > 0, \\ \frac{\partial\phi}{\partial x}(x_i, y_j) \approx \frac{1}{h}(-\frac{3}{2}\phi_{ij} + 2\phi_{i+1,j} - \frac{1}{2}\phi_{i+2,j}), & \text{if } \tilde{B}_x < 0. \end{cases} \tag{3.11}$$

$$\begin{cases} \frac{\partial\phi}{\partial y}(x_i, y_j) \approx \frac{1}{h}(\frac{3}{2}\phi_{ij} - 2\phi_{i,j-1} + \frac{1}{2}\phi_{i,j-2}), & \text{if } \tilde{B}_y > 0, \\ \frac{\partial\phi}{\partial y}(x_i, y_j) \approx \frac{1}{h}(-\frac{3}{2}\phi_{ij} + 2\phi_{i,j+1} - \frac{1}{2}\phi_{i,j+2}), & \text{if } \tilde{B}_y < 0. \end{cases} \tag{3.12}$$

3.3 Streamline Diffusion Finite Element Method (SD-FEM)

Following the streamline diffusion finite element method for boundary value problems [18, 26], we define

$$a_h(\phi, v) = a(\phi, v) + \sum_{\tau \in T_h} c_\tau(\kappa\Delta\phi + \tilde{\mathbf{B}} \cdot \nabla\phi + \tilde{C}\phi, \tilde{\mathbf{B}} \cdot \nabla v)_\tau, \quad \forall \phi, v \in V_h \tag{3.13}$$

and

$$b_h(\phi, v) = (\phi, v) + \sum_{\tau \in T_h} c_\tau(\phi, \tilde{\mathbf{B}} \cdot \nabla v)_\tau, \quad \forall \phi, v \in V_h, \tag{3.14}$$

where $(\cdot, \cdot)_\tau$ denotes the inner product in $L^2(\tau)$. In our computation, we choose $c_\tau = \mathcal{O}(h_\tau^2)$.

Our streamline diffusion finite element discretization for solving (3.5) is: Find $(H_h^{sd}, \phi_h^{sd}) \in R^1 \times V_h$ such that

$$a_h(\phi_h^{sd}, v) = H_h^{sd} b_h(\phi_h^{sd}, v), \quad \forall v \in V_h. \tag{3.15}$$

Remark 3.2 Let $\mathcal{T} : L^2(\Omega) \rightarrow V$ be defined by

$$a(\mathcal{T}f, v) = (f, v), \quad \forall v \in V \tag{3.16}$$

and $\mathcal{T}_h : L^2(\Omega) \rightarrow V_h$ be defined by

$$a_h(\mathcal{T}_h f, v) = b_h(f, v), \quad \forall v \in V_h. \tag{3.17}$$

Using the error estimates between \mathcal{T}_h and \mathcal{T} (see, e.g., [18, 26]) and the abstract spectral approximation results in [3], we are able to get the error estimates for (3.15) when the coefficients/parameters of (3.1) are of the same scale, too. However, this kind of error estimates are not very interesting since the problem we compute is convection-dominated.

Remark 3.3 As we mentioned before, SD-FEM is widely used in various problems such as diffusion-convection-reaction problems with convection dominant. But to our best knowledge, there is no work applying the streamline diffusion method to solve an eigenvalue problem. In fact, in some sense, the eigenvalue problems we discuss here can be regarded as nonlinear diffusion-convection-reaction problems with convection dominant. The nonlinearity obscures the regularity of solution, which makes it difficult to analyze the convergence of the numerical method.

3.4 Adaptive Streamline Diffusion Finite Element Method

To improve the computational efficiency, we combine the streamline diffusion finite element method with an adaptive method. Let T_h be a shape regular conforming triangular finite element mesh and ∂T_h the set of all interior edges (of elements) in T_h . We use the following a posteriori error estimators in our computation [31]:

$$\eta(\phi_h) = \left(\sum_{\tau \in T_h} A^{-1} h_\tau^2 \|R_\tau(\phi_h)\|_{0,\tau}^2 + \sum_{e \in \partial T_h} A^{\frac{1}{2}} h_\tau \|R_e(\phi_h)\|_{0,e}^2 \right)^{\frac{1}{2}}, \tag{3.18}$$

where

$$R_\tau(\phi_h) = H\phi_h - \kappa \Delta \phi_h - \tilde{B} \nabla \phi_h - \tilde{C} \phi_h \tag{3.19}$$

and

$$R_e(\phi_h) = \kappa \left[\frac{\partial \phi_h}{\partial \mathbf{n}} \right]_e \tag{3.20}$$

with $[\cdot]_e$ denoting the jump on the edge e .

Given a conforming mesh T_h , we apply the following refinement strategy [20, 30]:

- *Error estimation*

 Compute local error estimator

$$\eta_\tau(\phi_h) \equiv A^{-1} h_\tau^2 \|R_\tau(\phi_h)\|_{0,\tau}^2 + A^{\frac{1}{2}} \sum_{e \in \partial T_h, e \subset \bar{\tau}} h_\tau \|R_e(\phi_h)\|_{0,e}^2$$

for all $\tau \in T_h$.

• *Mark and local refinement*

Refine those elements $\{\tau\}$ that satisfy

$$\eta_\tau(\phi_h) > r \max_{\tau \in T^h} \eta_\tau(\phi_h), \tag{3.21}$$

where $r \in (0, 1)$ is a given refinement parameter.

In our computation, we use the triangle bisection approach [30] to refine the meshes.

To describe the adaptive finite element algorithm for (3.15), we shall replace the subscript h by an iteration counter k of the adaptive algorithm afterwards for convenience. Given an initial triangulation T_0 with size h_0 , we can generate a sequence of nested conforming triangulations T_k using the following loop:

Solve → Estimate → Mark → Refine.

More precisely, we have an adaptive finite element algorithm for (3.15) as follows:

Algorithm 3.1 Adaptive finite element algorithm

1. Pick an initial mesh T_0 and let $k = 0$.
2. Solve (3.15) on T_k and get the finite element eigenpair (H_k^{sd}, ϕ_k^{sd}) .
3. Compute local error indicators $\eta_\tau(\phi_k^{sd}) \forall \tau \in T_k$.
4. Refine such elements $\{\tau\}$ in T_k that satisfy

$$\eta_\tau(\phi_k^{sd}) > r \max_{\tau \in T_k} \eta_\tau(\phi_k^{sd}) \tag{3.22}$$

to get a new conforming mesh T_{k+1} , where $r \in (0, 1)$ is a given refinement parameter.

5. Let $k = k + 1$ and go to 2.

4 Numerical Results

In this section, we present numerical results using the above methods. First we give the results for the two dimensional cellular flow (1.3) and then the cat’s eye flow (1.4).

4.1 Numerical Results for the Cellular Flow

Using the above methods, we compute Eq. (3.1) under zero Neumann boundary condition in y . Figure 1 shows the numerical results using standard FEM, SD-FEM and upwind FDM with uniform meshes. Figure 2 shows those values in \ln (natural logarithm) function. We see from Fig. 2 that our results agree with the quarter law of speed growth. Figure 3 compares the adaptive SD-FEM with both uniform SD-FEM and uniform upwind FDM. We can see from the values of the front speed for $A = 1000$ in Fig. 3 that using the same degree of freedoms, the accuracy of the results using adaptive SD-FEM is much higher than that using uniform SD-FEM and uniform upwind FDM. Adaptive SD-FEM converges faster than the other two methods. Therefore adaptive SD-FEM is more efficient for the problem we compute. Comparing the results by uniform SD-FEM and uniform upwind FDM, uniform SD-FEM shows higher accuracy than uniform upwind FDM. Figure 4 compares the convergence rate of the front speed from adaptive SD-FEM with the rates from uniform SD-FEM and upwind FDM. We can see that the convergence rates of adaptive SD-FEM and upwind FDM are

Fig. 1 Front speed vs. flow amplitude of cellular flows using different discrete methods with uniform meshes

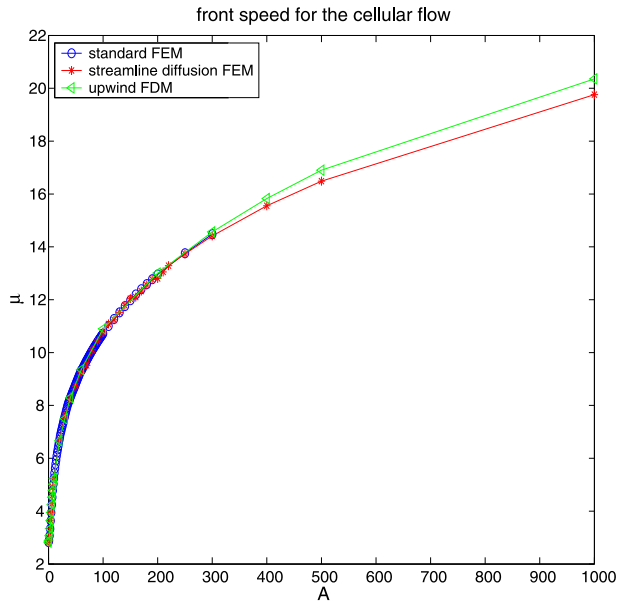
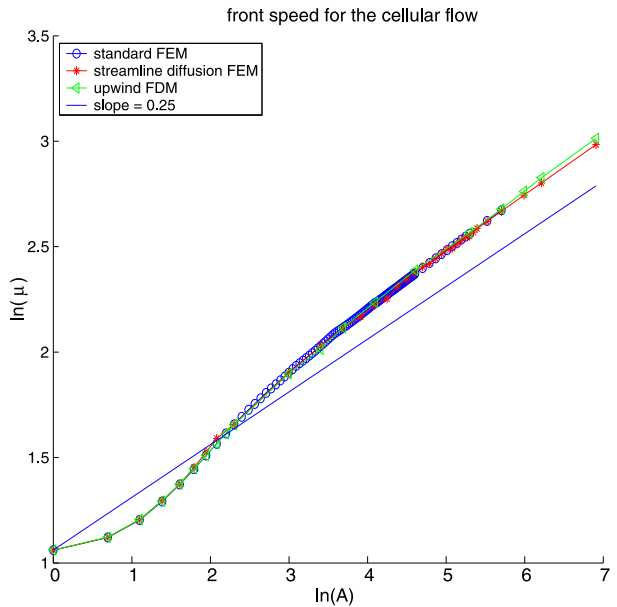


Fig. 2 The ln-ln plot of front speed vs. amplitude of cellular flow using different discrete methods with uniform meshes, recovering the quarter growth exponent



about 2, faster than that of uniform SD-FEM. Figure 5 shows the approximate front speed for $A = 1000$ and the corresponding adaptive mesh.

Figure 6 shows the values of $H(1)$ vs. A , suggesting that the growth of $H(1)$ is sublinear and above $O(A^{1/4})$ as known in theory [34].

Fig. 3 Numerical front speed convergence for cellular flow at amplitude $A = 1000$, using adaptive SD-FEM, uniform SD-FEM and uniform upwind FDM

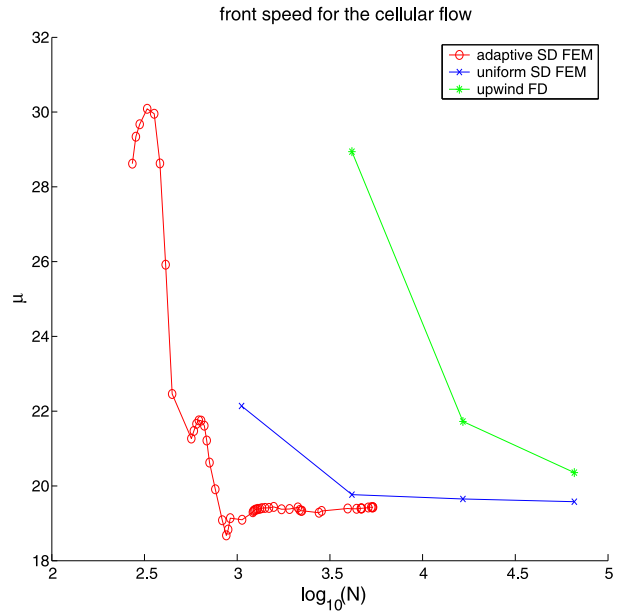
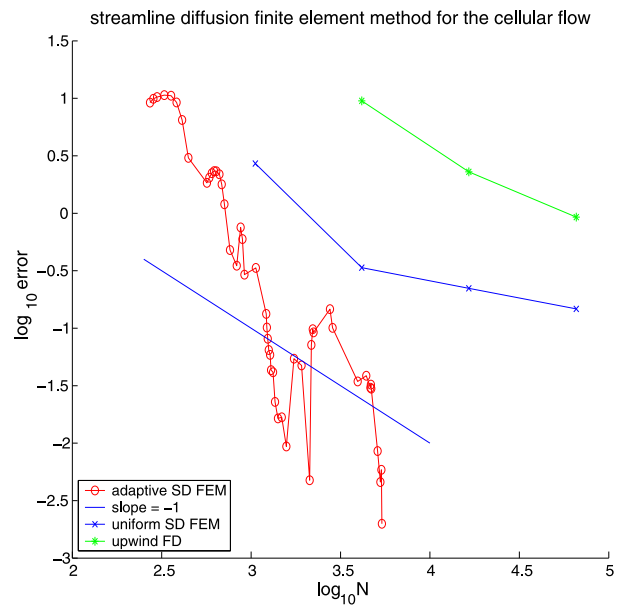


Fig. 4 The In-In plot of numerical front speed convergence for cellular flow at amplitude $A = 1000$, using adaptive method for $A = 1000$



4.2 Numerical Results for the Cat’s Eye Flow

In this subsection, we present the results for the cat’s eye flow with the perturbation parameter $\delta = 0.1, 0.2$. Since the boundary layer effect becomes significant when A increases, we use the uniform SD-FEM for $A < 400$ and the adaptive SD-FEM for $A \geq 400$ to improve

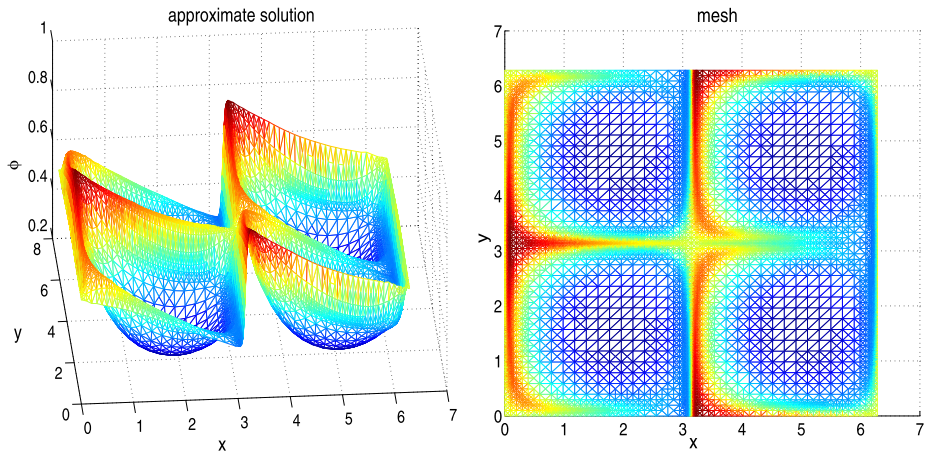


Fig. 5 The left figure shows the computational results of eigenfunction using the adaptive SD-FEM with $A = 1000$. The right figure shows the corresponding mesh

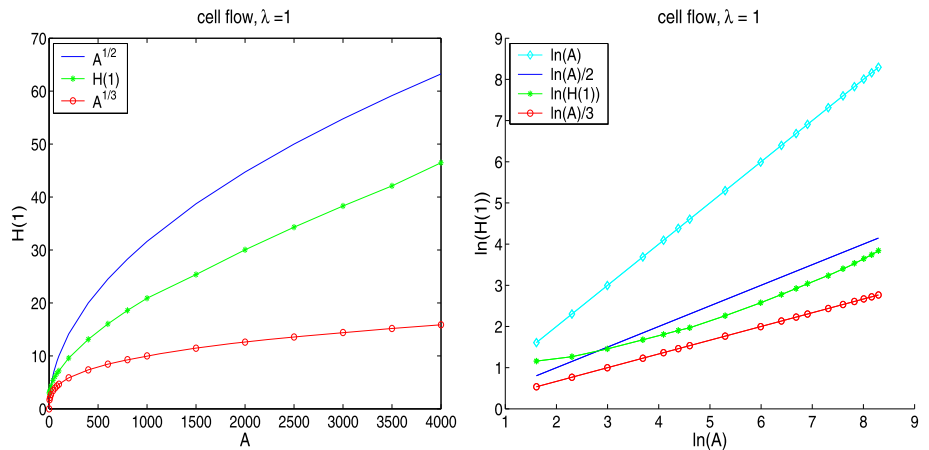


Fig. 6 The left figure show the values of $H(1)$. The right figure shows the values of $\ln(H(1))$

the accuracy. Figure 7 shows the vector fields for $\delta = 0.1, 0.2, 0.3$. The larger the δ values, the more opened the channels are.

We consider zero Neumann boundary condition in y for (3.1), and the scaled cat’s eye flow $\mathbf{B}(x, y) \rightarrow \mathbf{B}(kx, ky)$ with $k = 1, 5, 10, 15$. The results are shown in Fig. 8. To compare with the values for the cellular flows, we keep the data curves for the cellular flows in Fig. 8. Though growth exponent remains at 0.25, the speed values for cat’s eye flows are lower than those in cellular flows. It appears that zero Neumann boundary condition slows down the front speeds in cat’s eye flows even though open channels in them tend to increase the speeds. The boundary effect is the strongest for the unscaled cat’s eye flow $B(x, y)$ in that the speed curve is non-monotone and shows speed reduction in A as $A \geq 300$. The lower panels of Fig. 8 show that a larger δ value or more opening of the cat’s eye channels decreases

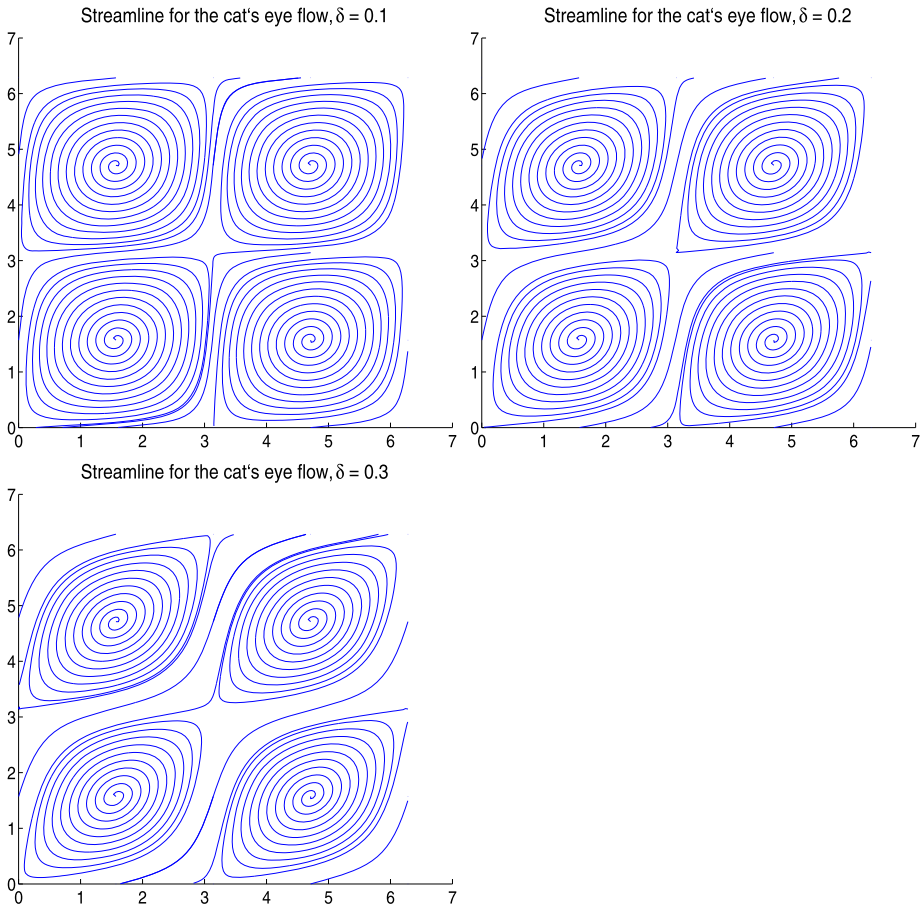


Fig. 7 The streamline for the cat's eye flow with $\delta = 0.1, 0.2, 0.3$

the speed at scale factor 1, 5, while increasing the speed at scale factor above 10. This phenomenon may be attributed to the zero Neumann boundary condition as well. Opening sufficiently many cat's eye channels is necessary to overcome the slow down effect of the no flux zero Neumann boundary condition in y . As we shall see in Fig. 9, opening cat's eye channels (by increasing δ) always increases speed if the periodic boundary condition is imposed in y . The computation becomes unstable for $B(x, y)$ and $\delta = 0.2$ when $A > 400$, though the trend is clear that the speed decreases in large A as in the case of $\delta = 0.1$. We shall study this regime further in the future.

Now we consider periodic boundary condition in y for (3.1) and the corresponding speed values in the cat's eye flows. The results are shown in Fig. 9. We see that the cat's eye flow in two dimensional periodic domain (both x and y) enhances more than cellular flows (exponents range 0.3–0.75 and are above 1/4) because of open streamlines along $(1, 1)$ from cell to cell. The growth exponent is theoretically 1 in the limit $A \rightarrow +\infty$ [34]. The exponents observed numerically here reflect the growth in the range of A values computed ($A \leq 1000$) which are still below the theoretical asymptotic regime. The slow-down with higher frequency (or more small scales) may be explained by the presence of more periodic structures

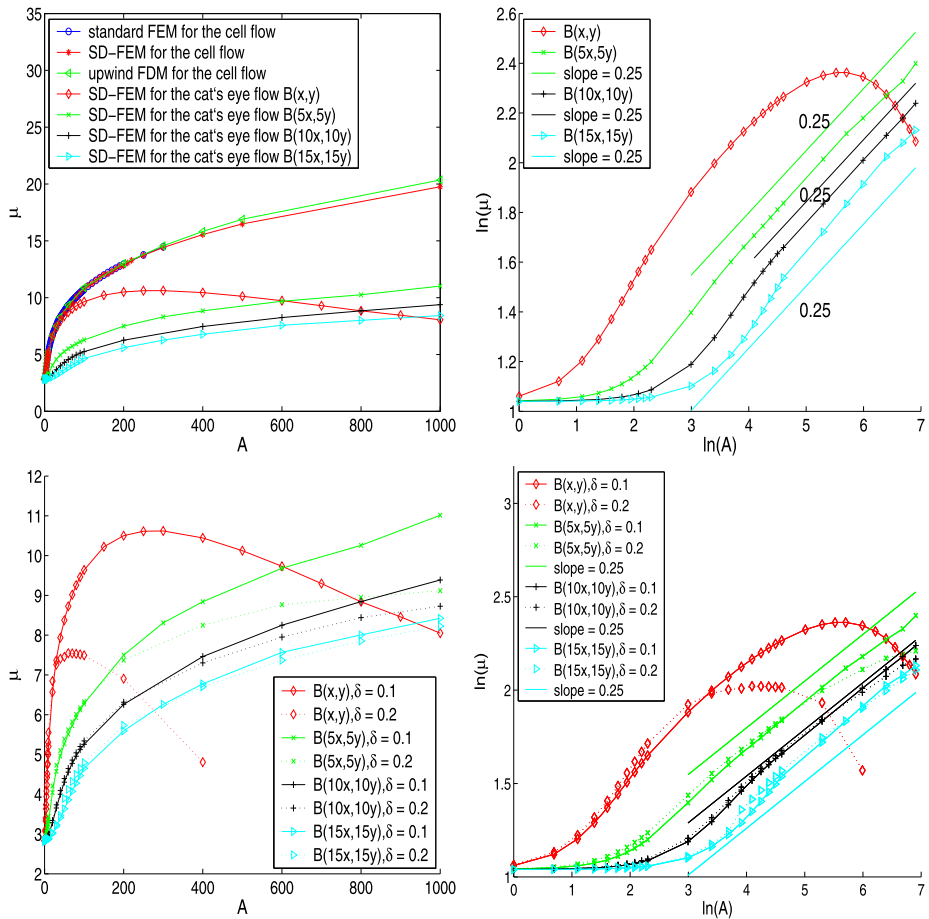


Fig. 8 The upper-left figure shows the numerical results for the cat’s eye flow and the scaled cat’s eye flow with perturbation parameter $\delta = 0.1$ using SD-FEM with periodic boundary condition in x direction and zero Neumann in y direction. The upper-right figure shows the ln-ln plot. The lower-left figure shows the results for the cat’s eye flow and the scaled cat’s eye flow with perturbation parameter $\delta = 0.1, 0.2$ with periodic boundary condition in x direction and zero Neumann in y direction. The lower-right figure shows the ln-ln plot

along the slow direction $(-1, 1)/\sqrt{2}$. Though there is help from fast direction $(1, 1)/\sqrt{2}$, front speed along $(1, 0)$ is still influenced more by the slow direction in the range of computed A values. The larger the cat’s eye parameter δ , the higher the growth exponents due to open channels being wider.

Remark 4.1 We can only compute with $A \in [0, 1000]$ due to the instability of the numerical methods. Exploring the enhancement laws for larger A requires much smaller size of the mesh, which leads to expensive computational cost. We will adopt parallel computation to improve the computational performance in the future work.

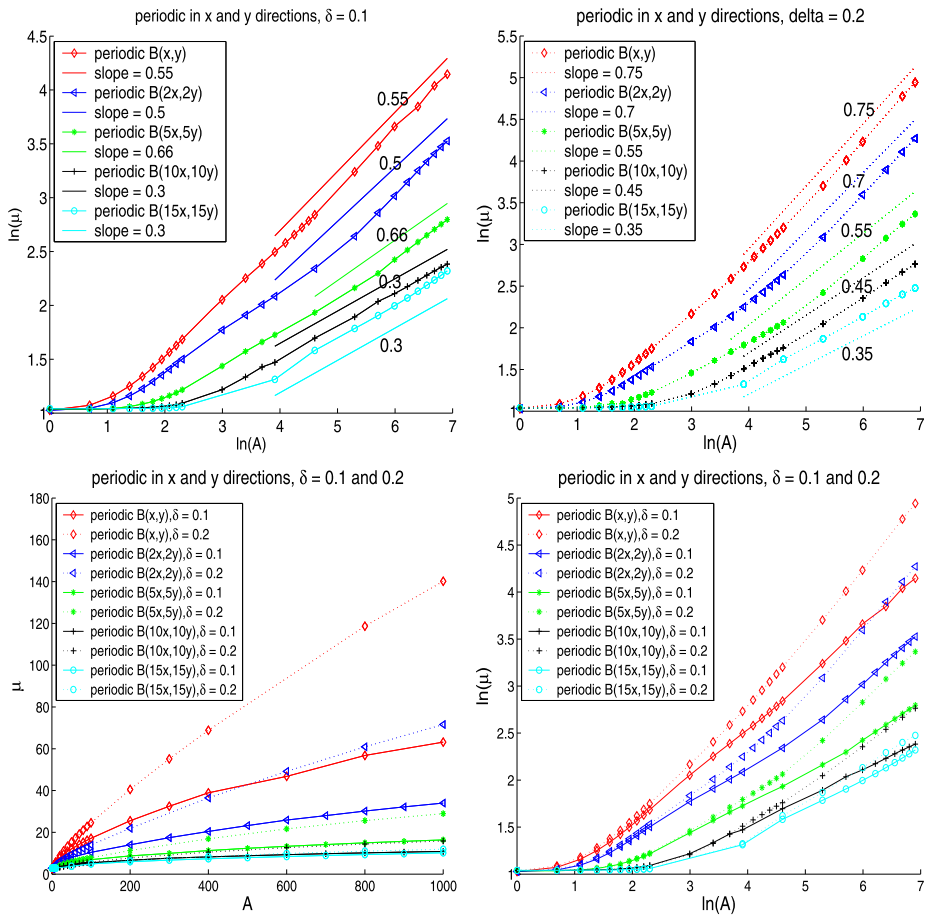


Fig. 9 The upper two figures show the numerical results for the cat’s eye flow and the scaled cat’s eye flows with perturbation parameter $\delta = 0.1$ and 0.2 . The results are obtained using SD-FEM with periodic boundary conditions in both x and y directions. The lower two figures put those data together and show the values of the speed and \ln values of them respectively

5 Concluding Remarks

We performed adaptive eigenvalue and KPP front speeds computation with finite element methods for both cellular flows and cat’s eye flows. Theoretical speed growth of cellular flows is recovered. New phenomena of fronts speed in cat’s eye flows are discovered: (1) slow down by zero Neumann boundary condition in the direction transverse to the front motion; (2) faster than the quarter growth law due to open channels in the cat’s eye flow; (3) slow down of the speed growth by higher frequencies of cat’s eye flows (or presence of more but smaller eddies of cat’s eye flows in the domain). In future work, we plan to adopt two-grid finite element method [28] and parallel computation to improve the computational efficiency so that we can deal with the instability for larger convection term. At the same time, we will compute KPP front speeds in three dimensional steady incompressible flows based on adaptive streamline diffusion finite element methods.

Acknowledgements LS was partially supported by National Science Foundation of China under grants 10801101, 10871198 and 11171232. JX was partially supported by NSF under grants DMS-0712881, DMS-0911277 and DMS-1211179. AZ was partially supported by the National Science Foundation of China under grants 10871198 and 10971059, the Funds for Creative Research Groups of China under grant 11021101, and the National Basic Research Program of China under grant 2011CB309703. LS would like to thank Dr. Zhiqiang Sheng at Beijing Institute of Applied Physics and Computational Mathematics for providing the Stabilized BICG solver. Part of the data are computed on the supercomputer O3800 in the Institute of Computational Mathematics and Scientific/Engineering Computing, Academy of Mathematics and Systems Science, Chinese academy of Sciences.

References

1. Abel, M., Cencini, M., Vergni, D., Vulpiani, A.: Front speed enhancement in cellular flows. *Chaos* **12**, 481–488 (2002)
2. Audoly, B., Berestycki, H., Pomeau, Y.: Réaction diffusion en écoulement stationnaire rapide. *C. R. Acad. Sci., Sér. 2, Méc. Phys. Chim. Astron.* **328**, 255–262 (2000)
3. Babuška, I., Osborn, J.E.: Eigenvalue problems. In: *Handbook of Numerical Analysis*, vol. II, pp. 641–787. North-Holland, Amsterdam (1991)
4. Babuška, I., Vogelius, M.: Feedback and adaptive finite element solution of one-dimensional boundary value problems. *Numer. Math.* **44**, 75–102 (1984)
5. Beattie, C.: Galerkin eigenvector approximations. *Math. Comput.* **69**, 1400–1434 (2000)
6. Berestycki, H., Hamel, F.: Front propagation in periodic excitable media. *Commun. Pure Appl. Math.* **55**, 949–1032 (2002)
7. Berestycki, H., Hamel, F., Nadirashvili, N.: Elliptic eigenvalue problems with large drift and applications to nonlinear propagation phenomena. *Commun. Math. Phys.* **253**, 451–480 (2005)
8. Bourlioux, A., Khouider, B.: Rigorous asymptotic perspective on the large scale simulations of turbulent premixed flames. *Multiscale Model. Simul.* **6**, 287–307 (2007)
9. Chen, Z.: Reservoir simulation: mathematical techniques in oil recovery. In: *CBMS-NSF Regional Conference Series in Applied Mathematics*, vol. 77. SIAM, Philadelphia (2007)
10. Chen, Z., Huan, G.-R., Ma, Y.: *Computational methods for multiphase flows in porous media*. In: *Computational Science and Engineering Series*, vol. 2. SIAM, Philadelphia (2006)
11. Childress, S., Soward, A.M.: Scalar transport and alpha-effect for a family of cat's eye flows. *J. Fluid Mech.* **205**, 99–133 (1989)
12. Clavin, P., Williams, F.: Theory of premixed-flame propagation in large-scale turbulence. *J. Fluid Mech.* **90**, 598–604 (1979)
13. Constantin, P., Kiselev, A., Oberman, A., Ryzhik, L.: Bulk burning rate in passive-reactive diffusion. *Arch. Ration. Mech. Anal.* **154**, 53–91 (2000)
14. Dai, X., Xu, J., Zhou, A.: Convergence and optimal complexity of adaptive finite element eigenvalue computations. *Numer. Math.* **110**, 313–355 (2008)
15. Eriksson, K., Johnson, C.: Adaptive streamline diffusion finite element methods for stationary convection-diffusion problems. *Math. Comput.* **60**, 167–188 (1993)
16. Fannjiang, A., Papanicolaou, G.: Convection enhanced diffusion for periodic flows. *SIAM J. Appl. Math.* **54**, 333–408 (1992)
17. Hughes, T.J.R., Brooks, A.N.: A multidimensional upwind scheme with no crosswind diffusion. In: Hughes, T.J.R. (ed.) *Finite Element Methods for Convection Dominated Flows*. ASME, New York (1979)
18. Johnson, C.: *Numerical Solution of Partial Differential Equations by the Finite Element Method*. Cambridge University Press, Cambridge (1987)
19. Majda, A., Souganidis, P.: Flame fronts in a turbulent combustion model with fractal velocity fields. *Commun. Pure Appl. Math.* **51**, 1337–1348 (1998)
20. Mao, D., Shen, L., Zhou, A.: Adaptive finite element algorithms for eigenvalue problems based on local averaging type a posteriori error estimates. *Adv. Comput. Math.* **25**, 135–160 (2006)
21. Nävert, U.: A finite element method for convection-diffusion problems. Ph.D. thesis, Chalmers University of Technology Göteborg (1982)
22. Nolen, J., Xin, J.: Computing reactive front speeds in random flows by variational principle. *Physica D* **237**, 3172–3177 (2008)
23. Novikov, A., Ryzhik, L.: Boundary layers and KPP fronts in a cellular flow. *Arch. Ration. Mech. Anal.* **184**, 23–48 (2007)
24. Peters, N.: *Turbulent Combustion*. Cambridge University Press, Cambridge (2000)

25. Ronney, P.: Some open issues in premixed turbulent combustion. In: Buckmaster, J.D., Takeno, T. (eds.) *Modeling in Combustion Science. Lecture Notes in Physics*, vol. 449, pp. 3–22. Springer, Berlin (1995)
26. Roos, H.-G., Stynes, M., Tobiska, L.: *Robust Numerical Methods for Singularly Perturbed Differential Equations. Springer Series in Computational Mathematics*, vol. 24, 2nd edn. (2008)
27. Ryzhik, L., Zlatos, A.: KPP pulsating front speed-up by flows. *Commun. Math. Sci.* **5**, 575–593 (2007)
28. Shen, L., Xin, J., Zhou, A.: Finite element computation of KPP front speeds in random shear flows in cylinders. *Multiscale Model. Simul.* **7**, 1029–1041 (2008)
29. Sivashinsky, G.: Cascade-renormalization theory of turbulent flame speed. *Combust. Sci. Technol.* **62**, 77–96 (1988)
30. Verfürth, R.: *A Review of a Posteriori Error Estimates and Adaptive Mesh-Refinement Techniques*. Wiley, New York (1996)
31. Verfürth, R.: Robust a posteriori error estimates for stationary convection-diffusion equations. *SIAM J. Numer. Anal.* **43**, 1766–1782 (2005)
32. Williams, F.: Turbulent combustion. In: Buckmaster, J. (ed.) *The Mathematics of Combustion*, pp. 97–131. SIAM, Philadelphia (1985)
33. Xin, J.: *An Introduction to Fronts in Random Media. Surveys and Tutorials in the Applied Mathematical Sciences*, vol. 5. Springer, Berlin (2009)
34. Xin, J., Yu, Y.: Analysis and comparison of large time front speeds in turbulent combustion models. (2011). [arXiv:1105.5607](https://arxiv.org/abs/1105.5607)
35. Yakhot, V.: Propagation velocity of premixed turbulent flames. *Combust. Sci. Technol.* **60**, 191–214 (1988)
36. Zlatos, A.: Sharp asymptotics for KPP pulsating front speed-up and diffusion enhancement by flows. *Arch. Ration. Mech. Anal.* **195**, 441–453 (2010)
37. Zlatos, A.: Reaction-diffusion front speed enhancement by flows. *Ann. Inst. Henri Poincaré, Anal. Non Linéaire* **28**, 711–726 (2011)